

Measurements of transverse forces on circular cylinders undergoing vortex-induced vibration

M. Branković¹, P.W. Bearman*

Department of Aeronautics, Imperial College, London SW7 2BY, UK

Received 27 September 2005; accepted 8 April 2006

Available online 28 July 2006

Abstract

Experiments have been carried out on a circular cylinder, with and without helical strakes, free to respond in a direction transverse to a water flow. The Reynolds number range was between 3×10^3 and 2.1×10^4 , the mass ratio was just above 0.8 and the fraction of critical damping was approximately 2×10^{-4} . Measurements are presented of the response, the transverse fluid force and the phase angle between the response and the force, all as a function of reduced velocity. The straked cylinder is observed to respond over a narrow range of reduced velocity and its maximum amplitude is decreased by just over 60%, compared with a plain cylinder. The familiar phase jump that occurs for a plain cylinder did not occur with the straked one, with the phase close to zero over the entire reduced velocity range where response to vortex shedding occurred.

© 2006 Elsevier Ltd. All rights reserved.

Keywords: VIV; Circular cylinders; Strakes; Transverse forces; VIV suppression

1. Introduction

Vortex-induced vibration (VIV) can severely limit the operation of structures and may even lead to catastrophic failure. Serious VIV problems can occur in air flows but particularly damaging events may take place in denser fluids such as water, and for the offshore industry, where the circular cylinder is such a common structural form, VIV presents an important and challenging problem. One of the essential requirements for predicting VIVs of circular cylinders is to have reliable data for flow-induced forces. It is not just the magnitude of the force that is required but also its phase relative to the motion. This information is often presented as the components of the force in-phase and out-of-phase with the displacement; with, respectively, one directly affecting oscillation frequency and the other oscillation amplitude [see for example Bearman (1984)].

Ideally, both in-line and transverse forces should be available and these need to be on hand as a function of Reynolds number, amplitude ratio and reduced velocity; there are other parameters such as surface roughness, aspect ratio and free-stream turbulence level which may also be important and affect response. Experimental and computational fluid dynamics (CFD) methods are available to determine these forces but both approaches are challenging. CFD-based methods developed to predict response require validation and, while this might be done by comparing calculated and

*Corresponding author. Tel.: +44 207 594 5055; fax: +44 207 584 8120.

E-mail address: p.bearman@imperial.ac.uk (P.W. Bearman).

¹Now at JP Kenny Pty, Perth, Western Australia

measured responses, it is valuable to have experimental data on fluid forces as an intermediate step. Such data is relatively scarce and in the case of circular cylinders is often found for only one-dimensional motion. For transverse forces on circular cylinders oscillating in the cross-flow direction there are data available for both free and forced motion, with the most comprehensive sets being for driven cylinders. Sarpkaya (1979) [see also Sarpkaya (2004)] has presented transverse force data for a range of amplitudes and reduced velocities. A further extensive set of data is available from Gopalkrishnan (1993). Transverse force data for a freely responding circular cylinder can be found, for example, in the work of Khalak and Williamson (1997). Hover et al. (2001) present force data for a circular cylinder driven via a novel electromechanical feedback system that simulates structural dynamics.

In this paper measurements of the transverse force acting on a freely vibrating circular cylinder, with low mass and low damping and constrained to move only in the cross-flow direction, are presented. The main purpose is to compare results for a plain circular cylinder and a cylinder fitted with helical strakes. The strakes are 3-start with a pitch of five diameters and a height equal to 10% of the bare cylinder diameter. At the low mass ratio used, the strakes were not sufficient to suppress VIV but they reduce the maximum amplitude, compared to the plain cylinder, by about 60%.

2. Experimental arrangement

The circular cylinder model used had a diameter of 68 mm and an immersed length of 584 mm, giving an aspect ratio close to 8.6. The cylinder was attached beneath a platform supported on a low damping, air bearing system that allowed motion only in a direction transverse to the flow. The structure supporting the air-bearings was fixed above a water channel which has a test-section 0.7 m deep, 0.6 m wide and 8.4 m long. The flow velocity could be increased up to 1 m/s

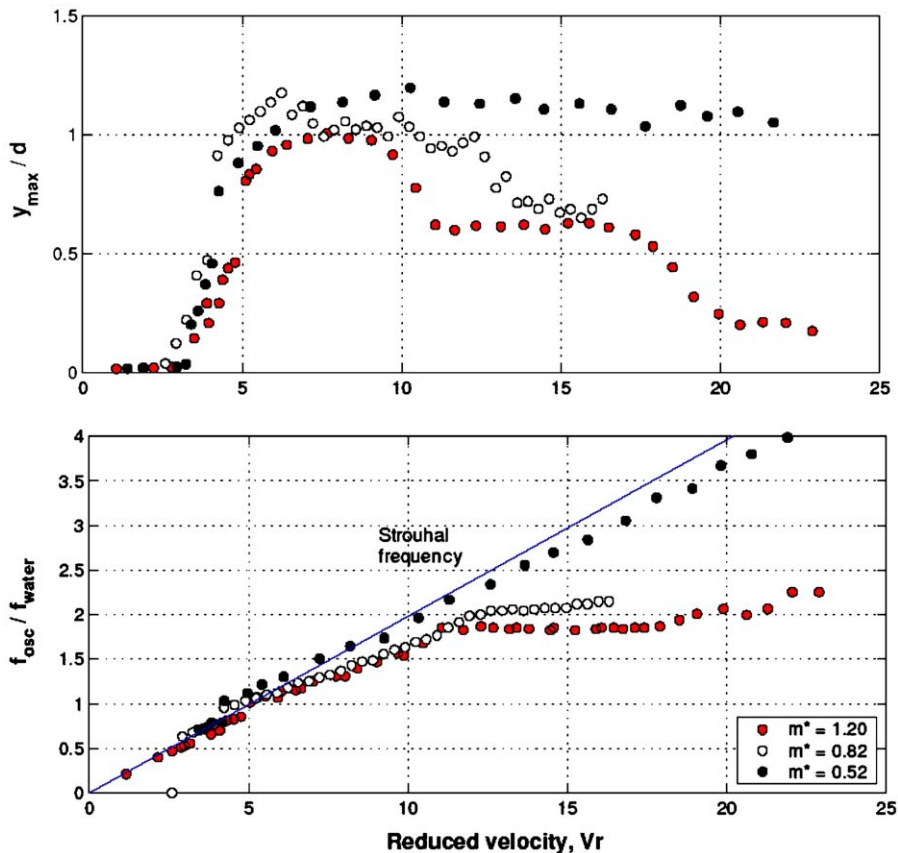


Fig. 1. Amplitude and oscillation frequency measurements versus reduced velocity for $m^* = 0.52$ and 1.2 (Govardhan and Williamson, 2000) and $m^* = 0.82$ (present results).

and the Reynolds number range for the results presented here is between 3000 and 21 000, based on cylinder diameter. The mass ratio m^* , effective mass of the cylinder/displaced mass of water, was 0.82 for the bare cylinder and 0.83 when it was fitted with strakes. Structural damping levels, ζ_s , varied between 1.5 and 2.5×10^{-4} , giving a typical value for $m^*\zeta_s$ of 1.6×10^{-4} . In this study the reduced velocity, V_r , is defined as $U/f_o d$, where U is channel flow velocity, d the bare cylinder diameter and f_o the oscillation frequency measured in air, which approximates to the natural frequency in a vacuum. In order to compare with other researchers, it should be noted that just in Fig. 1, f_o is replaced by f_{water} , the oscillation frequency in still water.

An optic fibre noncontacting sensor was used to measure the cylinder motion. To measure the unsteady transverse force a load cell was mounted between the cylinder model and the platform supported on the air bearings. In order to obtain the fluid force from the load cell reading, it was necessary to remove the inertia force associated with the cylinder model. In some further experiments a second set of cylinders was manufactured, with the same levels of mass and damping, which allowed dye to be introduced into the flow through small holes in the cylinder surface. The resulting visualization enabled the modes of vortex shedding to be identified. A hot-film probe was mounted downstream of the cylinders in order to obtain time histories of the flow velocity from which power spectra were obtained. Further details of the experimental arrangement, and the results, can be found in Branković (2004).

3. Experimental results

Fig. 1 shows a comparison of response data for the bare cylinder with earlier low mass and damping measurements by Govardhan and Williamson (2000) for values of m^* of 1.2 and 0.52, which straddle the present value of $m^* = 0.82$. It should be noted that Govardhan and Williamson used the oscillation frequency in still water, f_{water} , to nondimensionalise the oscillation frequency in flowing water, f_{osc} , and to form V_r . Plotted in Fig. 1 are the maximum amplitudes nondimensionalised by the cylinder diameter, d , and the oscillation frequencies versus reduced velocity. Given that the experiments were carried out totally independently and using different apparatus, the level of agreement is very encouraging.

Measurements for the plain cylinder of amplitude, phase, oscillation frequency and transverse force coefficient, C_y , together with its components in phase with the cylinder displacement, C_{ya} , and in phase with its velocity, C_{yu} , are plotted in Fig. 2 against reduced velocity. The modes of shedding observed are given in the top left hand plot of amplitude versus reduced velocity. The two vertical lines in the figure correspond to $V_r = 2.9$, where the transverse force coefficient is a maximum, and $V_r = 5.4$ where the oscillation frequency coincides with the natural frequency, i.e. $f_{\text{osc}} = f_o$. In analyses of VIV it is often assumed that both the response and the force can be approximated to sine waves displaced by a phase angle ϕ . Using this assumption leads to the following expression for the phase,

$$\phi^\circ = \tan^{-1} \left[\frac{2\zeta_s \frac{f_{\text{osc}}}{f_o}}{1 - \left(\frac{f_{\text{osc}}}{f_o}\right)^2} \right].$$

In Fig. 2 the phase angle is calculated using this relation. For the low mass ratio employed here ϕ is either close to 0° or 180° and, as can be seen from the above expression, will switch between the two when $f_{\text{osc}} = f_o$ or, alternatively, when the added mass changes sign. The assumption that time traces can be represented by sine waves was found to be valid at some reduced velocities but significant amplitude and frequency modulation was observed in the range of V_r where there appeared to be intermittent modes of shedding. C_{yu} and C_{ya} were calculated by taking a time average of the products of the instantaneous transverse force with the cylinder displacement and the cylinder velocity, respectively. It can be seen that the maximum value of C_y , and the peak magnitudes of its components, occur at $V_r = 2.9$ and this is in a regime where the mode of shedding is 2S.

Power spectra of the displacement (f_{osc}), the transverse force (f_{lift}) and the output from a hot-film probe placed downstream of the cylinder (f_{shedding}) are plotted together in Fig. 3 for six values of the reduced velocity. These six values are marked by the open circles in Fig. 2. Displacement has a sharply-tuned spectrum throughout the V_r range whereas the transverse force only displays a narrow band response in the 2S and 2P modes. In general the spectra for the hot-film output follow those of the transverse force. In what has been referred to as the intermittent mode in Fig. 2, the transverse force, which is the fluid force acting on the whole cylinder, appears to be quite broad-band and this may be the result of mode switching and instantaneous variations of the transverse force along the span. Hover et al. (2002) observed a lack of spanwise correlation of the transverse force in a similar range of V_r .

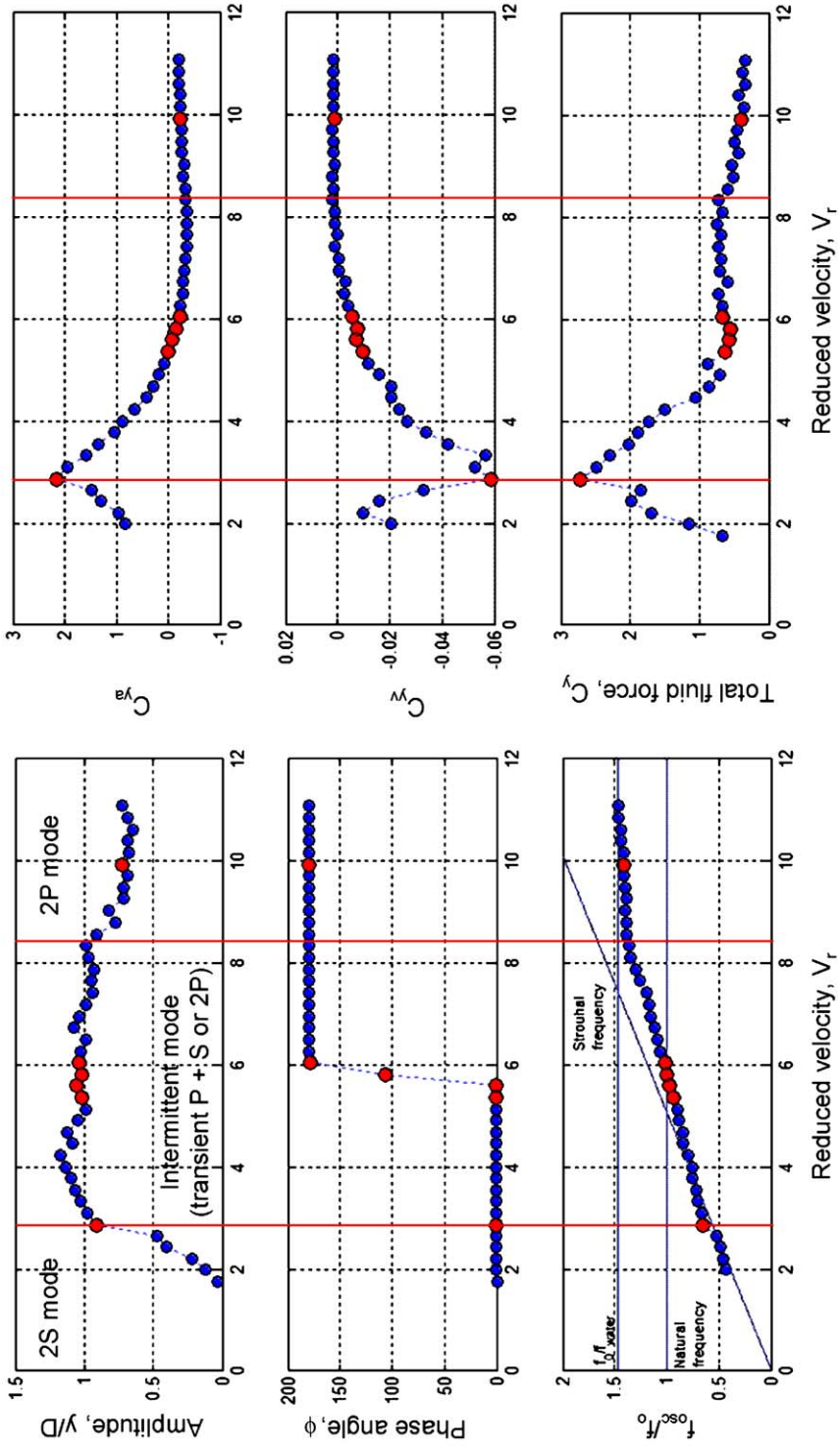


Fig. 2. Response and transverse force measurements for a plain cylinder with $m^* = 0.82$ and $\zeta_s = 1.5 \times 10^{-4}$.

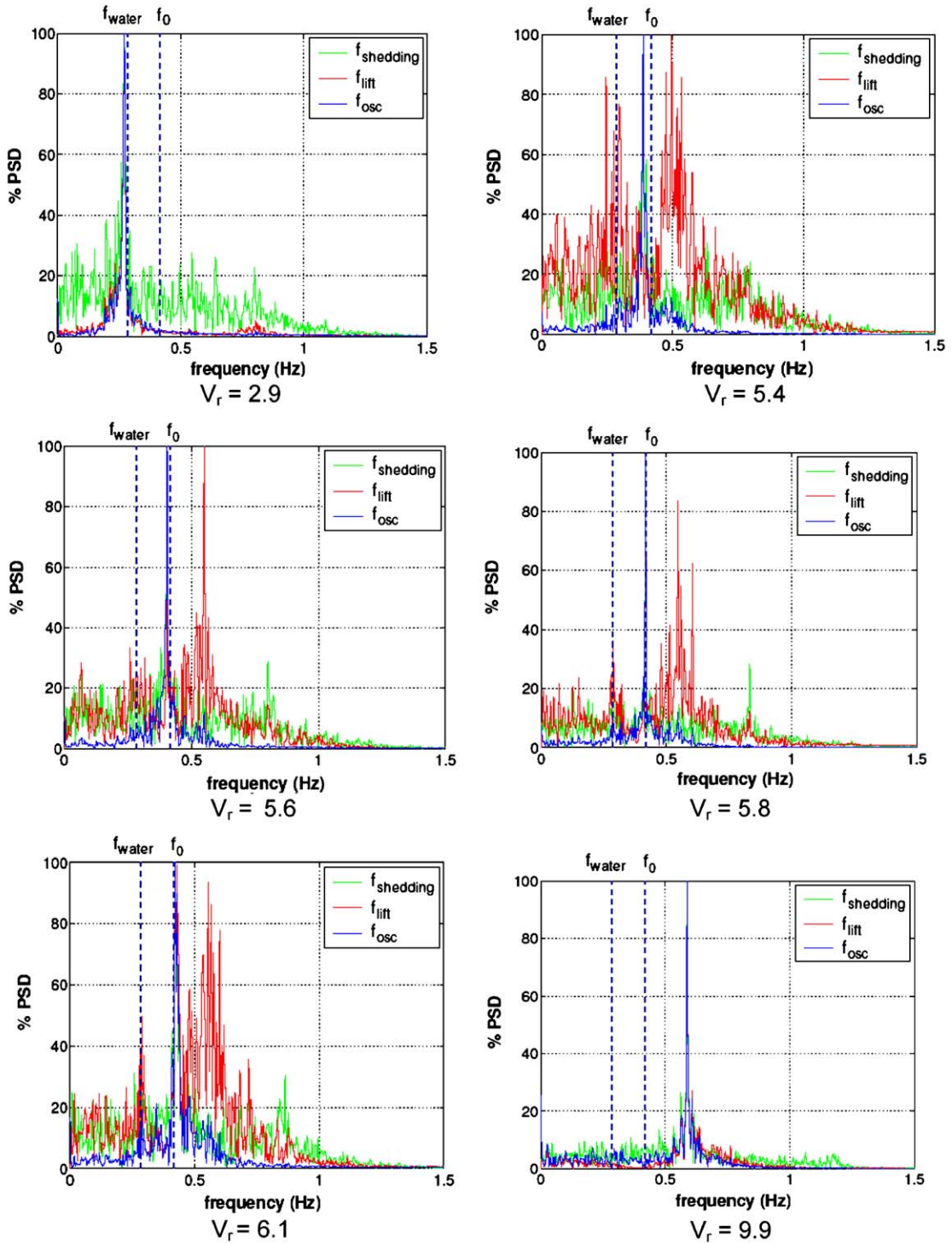


Fig. 3. Plain cylinder showing spectra of response, transverse force and wake velocity.

Corresponding results for the cylinder fitted with strakes are shown in Figs. 4 and 5. The first point to note is that the range of VIV response is small and is between reduced velocities of about 3 and 5. The general form of the transverse force with V_r is similar to that for the plain cylinder, with the maximum value again occurring at around $V_r = 2.9$; but

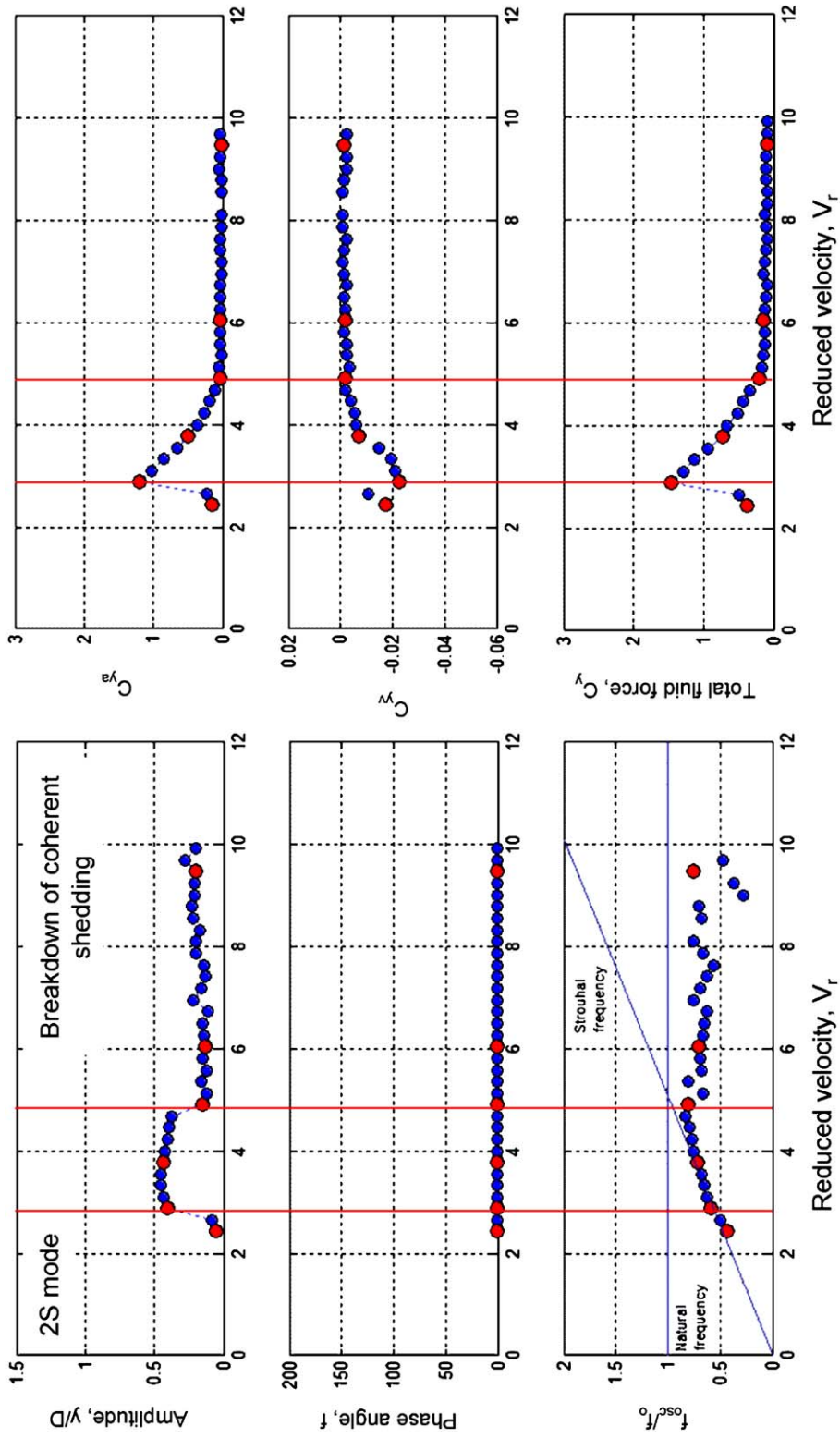


Fig. 4. Response and transverse force measurements for a straked cylinder with $m^* = 0.83$ and $\zeta_s = 2.5 \times 10^{-4}$.

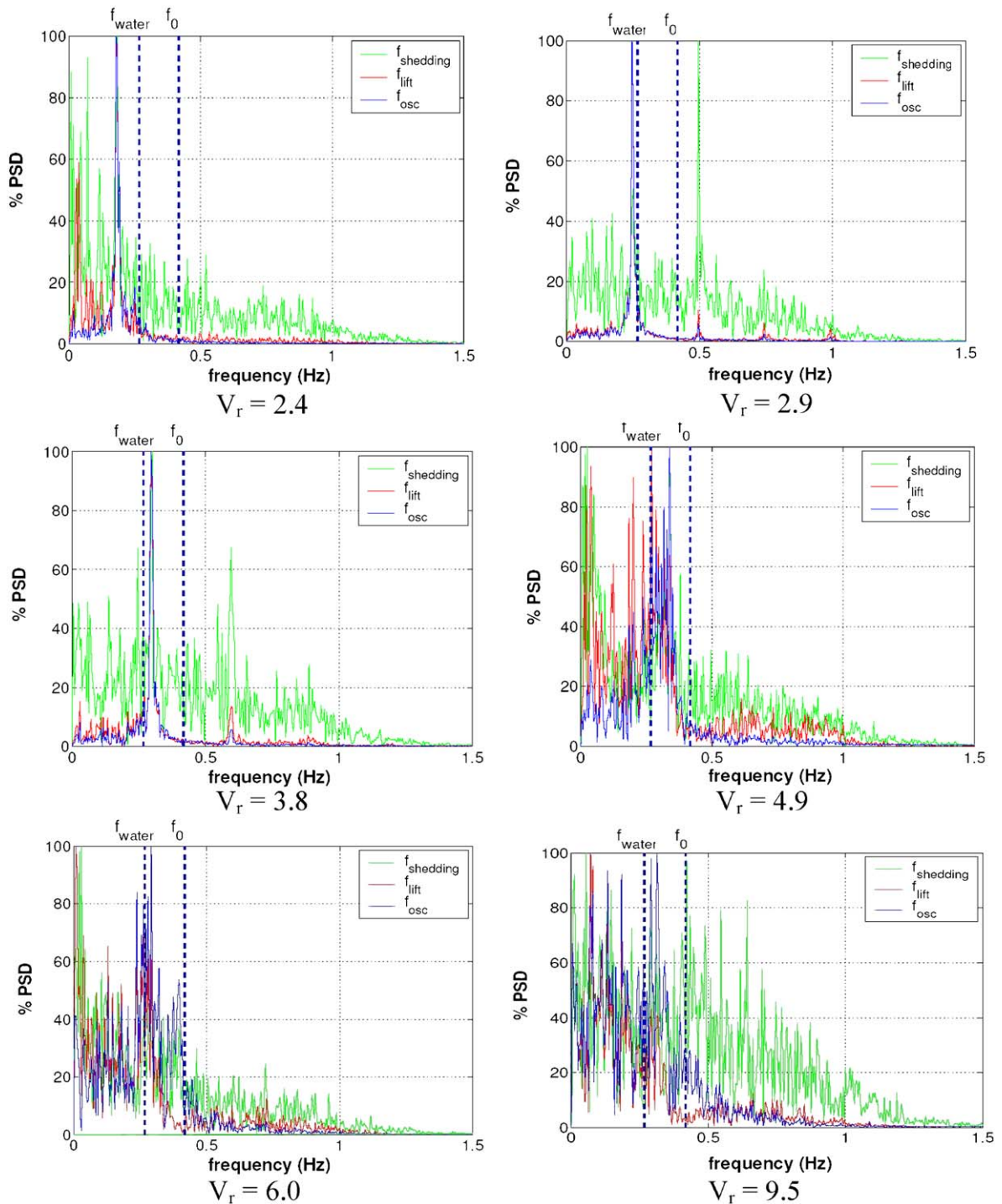


Fig. 5. Straked cylinder showing spectra of response, transverse force and wake velocity.

whereas the strakes reduce the maximum amplitude by about 63%, the force is only reduced by just under 50%. However, perhaps the most interesting feature is that the oscillating frequency never exceeds the natural frequency and the switch in shedding phase observed for plain cylinders does not take place. Coupled with this finding is that the added mass for a straked cylinder remains positive throughout the V_r range.

Visualization of the flow close to the surface of the straked cylinder indicated strong three-dimensionality with fluid being directed along the strakes. It was observed that flow separated at some locations from the tip of a strake and at others from the smooth surface of the cylinder. Separation from a strake was accompanied by strong shear layer curvature, and small vortices developed in the shear layer, similar to those first observed for circular cylinder flow by Bloor and Gerrard (1966). In some earlier work on straked cylinders, Bearman and Branković (2004) visualized the flow for a cylinder with $m^* = 1.47$ and, as V_r increased, they first observed the 2S mode and then what appeared to be the 2P mode. Visualisation in the present study with $m^* = 0.83$ again showed the 2S mode but no distinct 2P could be found. Clearly more work is required to determine the influence of mass ratio on shedding modes for a straked cylinder.

4. Conclusions

Transverse force measurements on freely vibrating plain and straked circular cylinders have been made for very low damping and a mass ratio of about 0.8. For the plain cylinder the response is in good agreement with previous measurements. Spectra of the transverse force show the signal to be spread across a broad band of frequencies in the upper branch, whereas the response remains in a narrow-band. When there are clear 2S and 2P modes the force and the response are both narrow-band and centred on the same frequency. In a range of V_r between about 3 and 5 the straked cylinder responds with an amplitude about 60% less than that for the plain cylinder. The familiar phase jump that occurs for a plain cylinder does not take place on a straked cylinder and the phase angle remains close to zero throughout.

Acknowledgement

One of the authors, MB, was in receipt of a research studentship and wishes to acknowledge the support of the Engineering and Physical Sciences Research Council.

References

- Bearman, P.W., 1984. Vortex shedding from oscillating bluff bodies. *Annual Review of Fluid Mechanics* 16, 195–222.
- Bearman, P.W., Branković, M., 2004. Experimental studies of passive control of vortex-induced vibration. *European Journal of Mechanics B* 23, 9–15.
- Branković, M., 2004. Vortex-induced vibration attenuation of circular cylinders with low mass and damping. Ph.D. Thesis, University of London, UK.
- Gopalkrishnan, R., 1993. Vortex induced forces on oscillating bluff cylinders. Ph.D. Thesis, Department of Ocean Engineering, MIT, Cambridge, MA, USA.
- Govardhan, R., Williamson, C.H.K., 2000. Modes of vortex formation and frequency response of a freely vibrating cylinder. *Journal of Fluid Mechanics* 420, 85–130.
- Hover, F.S., Tvedt, H., Triantafyllou, M.S., 2001. Vortex-induced vibrations of a cylinder with a tripping wire. *Journal of Fluid Mechanics* 448, 175–195.
- Hover, F.S., Davis, J.T., Triantafyllou, M.S., 2002. Is mode transition three-dimensional? Conference on Bluff Body Wakes and Vortex-Induced Vibrations (BBVIV3), 17–20 December, Port Douglas, Australia.
- Khalak, A., Williamson, C.H.K., 1997. Fluid forces and dynamics of a hydroelastic structure with very low mass and damping. *Journal of Fluids and Structures* 11, 973–982.
- Sarpkaya, T., 1979. Vortex-induced oscillations. *Journal of Applied Mechanics* 46, 241–258.
- Sarpkaya, T., 2004. A critical review of the intrinsic nature of vortex-induced vibrations. *Journal of Fluids and Structures* 19, 389–447.